Interpretation of Contrast-Enhanced Mammography

4

Marc Lobbes

4.1 Introduction

Contrast-enhanced mammography (CEM) is most commonly performed in women who have clinical symptoms, a contraindication for breast MRI, or abnormal screening mammograms requiring additional imaging. A typical CEM exam consists of three different images per breast and per view: low-energy, high-energy, and recombined. As in conventional full-field digital mammography (FFDM), both breasts should be imaged in two standard views (i.e., craniocaudal and mediolateral oblique views). Additional views (e.g., magnification, spot compression, and rolled views) can be requested by the radiologist if necessary and can be acquired when performing CEM. A typical example of a standard CEM exam is presented in Fig. 4.1.

4.2 Contrast-Enhanced Mammography Images

4.2.1 Low-Energy Images

The low-energy images are acquired at least 2 min after the completion of intravenous administration of an iodine-based contrast agent, usually at a dose of ≥300 mg/ml. Although the breast tissue already contains contrast, it cannot be appreciated visually as these images are acquired at keV levels below the *k*-edge of iodine. Several studies have compared low-energy images with conventional FFDM images.

Fallenberg et al. compared FFDM and CEM in 118 women with histologically proven breast cancer [1]. Sensitivity across readers increased from 77.9% for FFDM

M. Lobbes (✉)
Department of Radiology and Nuclear Medicine, Maastricht University Medical Center, Maastricht, The Netherlands
e-mail: marc.lobbes@mumc.nl

M. Lobbes, M. S. Jochelson (eds.), *Contrast-Enhanced Mammography*,
https://doi.org/10.1007/978-3-030-11063-5_4

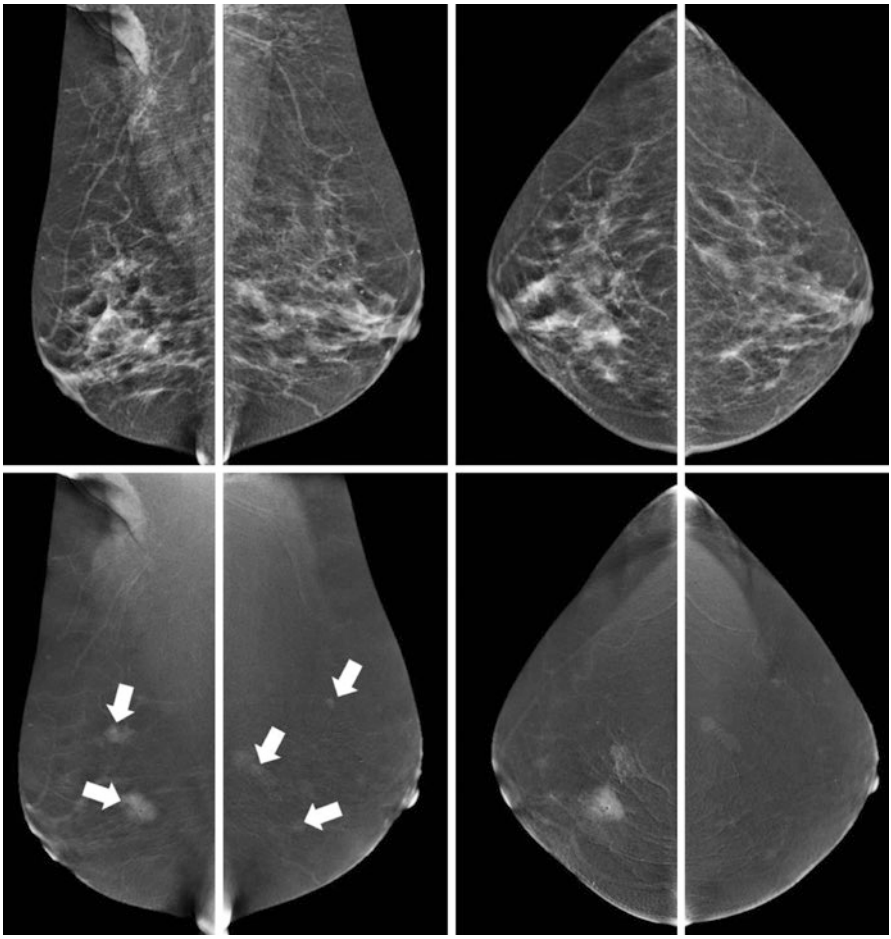

Fig. 4.1 Typical example of a standard contrast-enhanced mammography exam, consisting of low-energy images (top row) and recombined images (bottom row). Images are acquired from both breasts in the standard mammographic views (craniocaudal and mediolateral oblique). In this case, bilateral multifocal invasive breast cancer was diagnosed (arrows)

to 94.7% for CEM. This did not improve any further by adding a separate mammogram. Regarding tumor size, CEM resulted in a slight overestimation of 0.6 mm, whereas the combination of CEM and FFDM resulted in an overestimation of 4.5 mm. Hence, the authors concluded that FFDM is not necessary if CEM has been performed.

Francescone et al. compared low-energy CEM with FFDM images of 170 breasts. In this study, 88 women had both CEM and FFDM within 6 months of each other while undergoing evaluation for newly diagnosed breast cancer or screening [2]. The study parameters included mammographic findings such as calcifications and masses, distance from the nipple to chest wall, compression

thickness, and compression force on the mediolateral oblique view. The authors concluded that the low-energy CEM images were equivalent to the FFDM images, as they did not observe any statistically significant differences regarding the study parameters.

Lastly, Lalji et al. studied the similarity of low-energy CEM and FFDM on both a breast phantom and in clinical cases [3]. For the phantom experiments, they did not find any significant difference between detection thresholds for CEM and FFDM at different phantom thicknesses using a CDMAM phantom and by applying CEM settings commonly used in clinical cases. After the phantom study, two experienced radiologists compared the quality of CEM and FFDM images in 147 women who underwent both CEM and FFDM within 2 weeks of each other. Images were scored according to the European Reference Organization for Quality Assured Breast Screening and Diagnostic Services [4]. Of the 20 scoring criteria, no statistically significant differences were found in 17 criteria. Two criteria determined that there was superior visualization of (micro)calcifications on the low-energy images, although these differences were small ($p = 0.042$). These differences were also not confirmed by the previous study by Francescone et al. [2]. The delineation of the pectoral muscle on mediolateral oblique views was considered worse on low-energy CEM exams ($p < 0.001$), but the authors concluded that this would not cause any clinically relevant limitations.

Based on these three studies, it is safe to conclude that low-energy images are equivalent to FFDM.

4.2.2 High-Energy Images

The high-energy images are acquired within seconds of the low-energy images and primarily used for imaging the areas of iodine uptake, as these are acquired with keV levels above the *k*-edge of iodine. As the energy of the X-ray spectrum used is much higher, less radiation is absorbed when passing through the breast tissue. The high-energy images result in only a small additional radiation dose to the breast. The high-energy images are white and not suitable for any form of interpretation. The data in these images are used in conjunction with that of low-energy images to construct the recombined CEM images.

4.2.3 Recombined Images

The recombined images provide images of areas of enhancement enabled by increased perfusion of the breast tissue at the site of a malignant or occasionally benign neoplasm. In clinical practice, the radiologist views the low-energy and recombined images of both breasts in at least two views. Although the recombined images are reconstructed from images which are acquired only seconds apart, some artifacts can be observed. The radiologist evaluating CEM images should be aware of these artifacts, as knowledge of them reduces clinical dilemmas.

4.2.4 Artifacts on Recombined Images

The most common artifacts on recombined images are "breast-in-breast" artifacts; artifacts caused by breast implants, medical devices, or jewelry; ripple or motion artifacts; axillary line artifacts; and skin line enhancement artifacts.

The "breast-in-breast" artifact consists of a band of lower gray values at the periphery of the breast, simulating a double breast contour (Fig. 4.2). The artifact is observed in approximately 95% of images but usually does not result in difficulties in image interpretation [5]. This artifact is produced by different patterns of scatter radiation in low- and high-energy CEM images. These are assumed to be similar during reconstruction to form a recombined image, but this is not entirely true. The artifact is most pronounced in larger breasts and is commonly seen with first-generation CEM units, as the anti-scatter grids used then were not specifically designed for high-energy acquisitions. With next-generation CEM units, this artifact is less pronounced.

Women with breast implants are difficult to image with CEM. The implants create extensive artifacts on recombined images. The physics behind CEM is based on the presence of breast tissue (i.e., fat and fibroglandular tissue) and iodine.

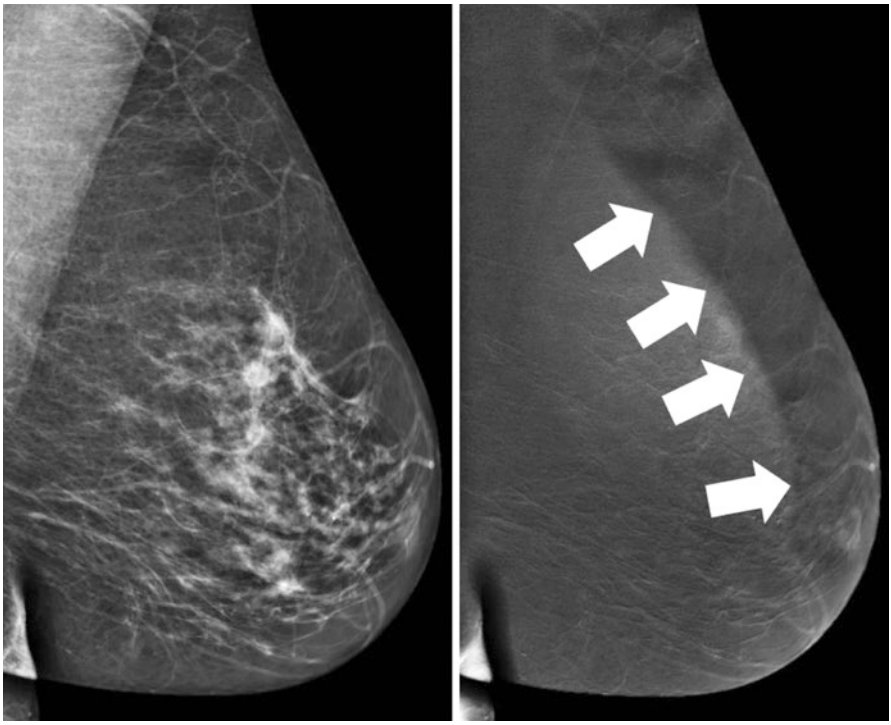

Fig. 4.2 Example of the "breast-in-breast" artifact. On the recombined images, a band of lower gray values can be observed at the periphery of the breast, suggesting a double breast contour (arrows)

Consequently, the distinction of breast tissue with material of any other composition, such as silicone or metal, would require an extra third acquisition with a different X-ray spectrum, leading to more noise in the recombined images. Similarly, other medical devices or jewelry (such as piercings) create artifacts on the recombined images (Fig. 4.3). Although CEM can be performed in women with medical devices or jewelry, the breast tissue surrounding these can only be evaluated on low-energy images. Hence, women with jewelry should be encouraged to remove these prior to CEM if possible.

The ripple artifact consists of fine black and white lines arranged in a ripple-like fashion layered upon the breast tissue (Fig. 4.4). It is observed in approximately 32% of cases [5]. Jeukens et al. found that although low- and high-energy images are acquired within seconds apart, the (mean) image acquisition time is 1.4 s for low-energy images compared with 4.2 s for high-energy images [6]. Therefore, in this time frame, slight motion from a patient could create a "mismatch" between the images in the post-processing of the recombined image. As a result, ripple artifacts are most often seen in the mediolateral oblique view, since the compression of the breast is then more centered on the upper part of the breast and the pectoral muscle,

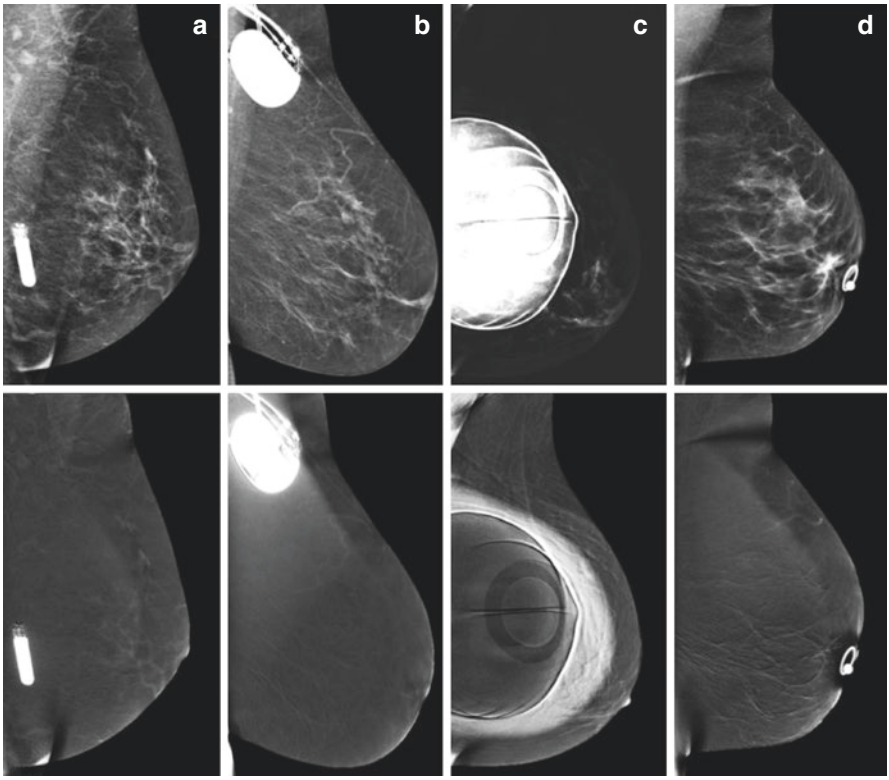

Fig. 4.3 Artifacts caused by cardiac devices, breast implants, or jewelry. Examples of (**a**) implantable cardiac monitoring device, (**b**) cardiac pacemaker, (**c**) breast implant, and (**d**) nipple piercing

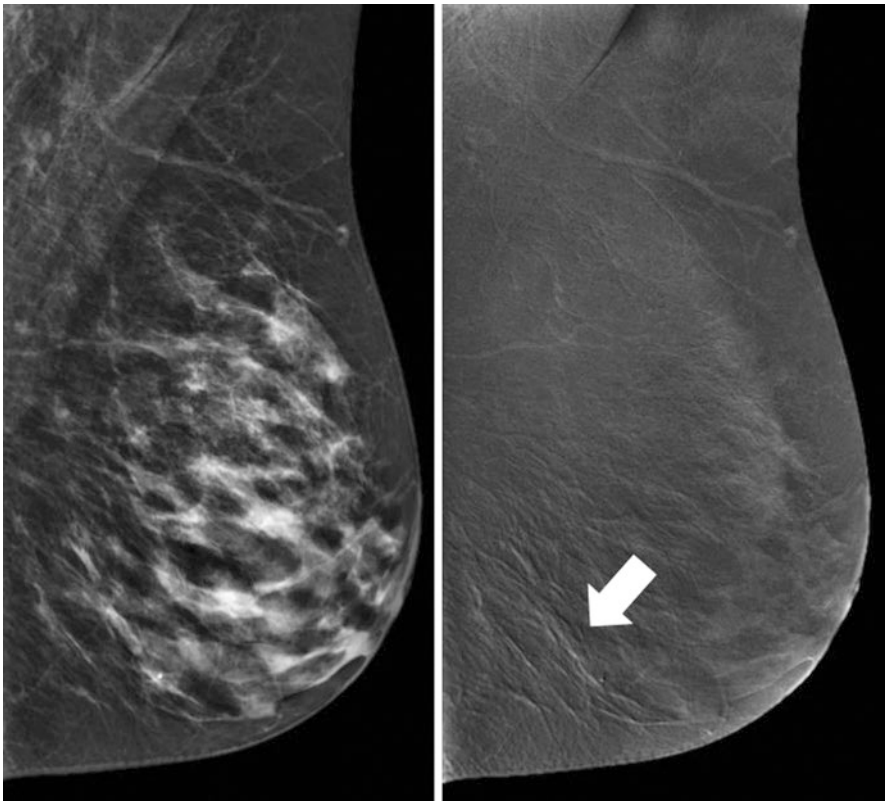

Fig. 4.4 Example of the ripple artifact. The ripple artifact consists of fine black and white lines in a ripple-like fashion layered upon the breast tissue and is caused by slight motion of the patient between the acquisition of the low-energy and high-energy CEM image

while the lower parts of the breast are usually less effectively compressed, rendering them susceptible to slight motion. To reduce ripple artifacts, some institutes recommend breath-holding instructions during the image acquisition phase.

The axillary line artifact consists of a well-defined line extending across the axillae and occurs in approximately 32% of images (Fig. 4.5). It is only observed on mediolateral oblique views and is always bilateral [5]. Usually, there is no interference with image interpretation. This artifact occurs due to the high sensitivity of high-energy images to lag. The line corresponds to the collimator position in previously acquired collimated images.

The skin line enhancement artifact consists of a segmental area of skin contour highlighting (Fig. 4.6). It does not involve the entire skin. It is presumably caused by image filtration which is applied to the recombined image to equalize breast thickness. When no apparent skin abnormalities are present, such as skin thickening, the skin line enhancement artifact is the most probable cause of the finding. It occurs in approximately 32% of cases and is mostly seen in the craniocaudal views [5].

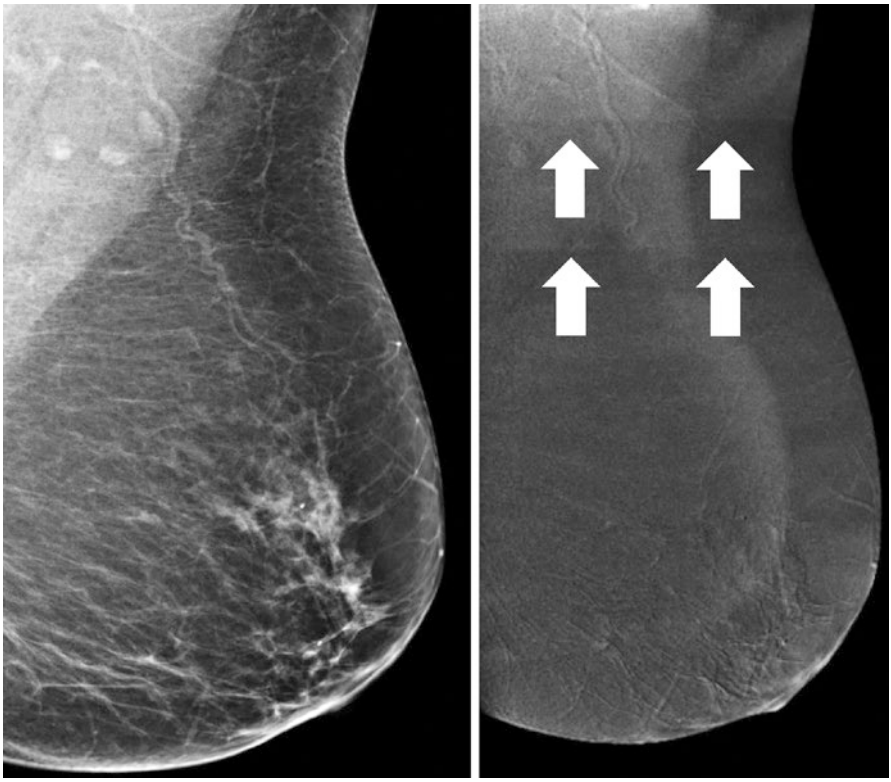

Fig. 4.5 Example of the axillary line artifact (arrows). An ill-defined line is present extended through the axilla. Images courtesy of Miriam Sklair-Levy, MD

In general, these artifacts do not present any relevant difficulties in image interpretation when the radiologist is familiar with them. It should also be noted that these artifacts are largely based on initial experiences with the first available CEM unit (SenoBright*) brought to market by GE Healthcare. In other commercially available units or newer generation models, these artifacts might be less prominent or even absent due to improvements in both hardware and software.

4.3 Image Interpretation

4.3.1 How to Read the Low-Energy Image

As discussed above, low-energy images are the CEM counterpart of FFDM images. Hence, they can be evaluated using a similar approach and terminology as suggested in the American College of Radiology Breast Imaging Reporting and Data System (BI-RADS) lexicon [7]. Although a detailed description of this evaluation is beyond the scope of this chapter, a summary is provided below.

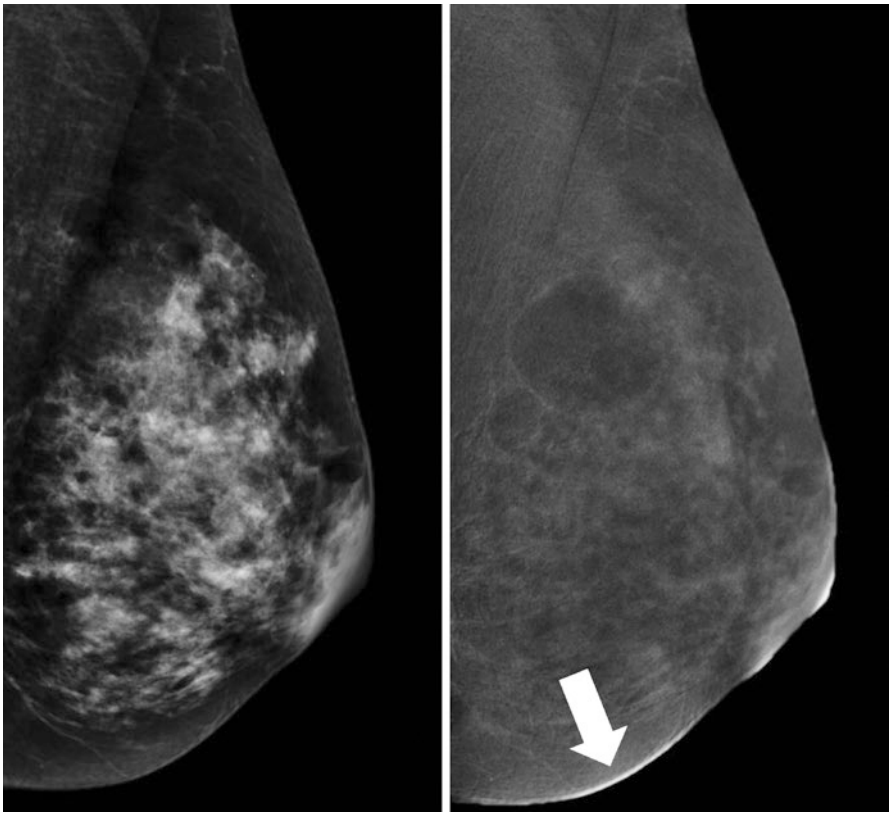

Fig. 4.6 Example of skin line enhancement artifact (arrow). There is a focal skin contour highlighting present on the recombined images (only left mediolateral oblique view shown) without any accompanying skin thickening or abnormality present on the low-energy image

As in any mammographic exam, an overview of the exams performed and the quality of the image acquisition (in terms of positioning, etc.) should be described, including the availability of any prior exams. As a first step, a description of the breast density should be provided in the report according to four different categories: (1) almost entirely fat, (2) scattered fibroglandular tissue, (3) heterogeneous fibroglandular tissue, or (4) extreme fibroglandular tissue. Although the accuracy of CEM is less influenced by breast density than FFDM, it remains important to report on breast density as this is reflective of the risk of developing breast cancer. In addition to the subjective classification of breast density ("eyeballing") which is less reliable [8], different (semi-)automated classification tools have been developed.

For the detection of breast abnormalities, four main categories can be distinguished: masses, architectural distortion, asymmetry, and (micro)calcifications. For each of these items, the nomenclature of the BI-RADS lexicon should be applied for the report. In addition, the lesion size and location within the breast should be reported. Finally, any clinically relevant additional findings such as benign

calcifications, vascular calcifications, skin abnormalities, axillary lymphadenopathy, etc. may be reported. For more specific details on state-of-the-art reporting of mammographic images, the BI-RADS lexicon can be consulted [7].

4.3.2 How to Read the Recombined Image

The recombined image should be evaluated in conjunction with the low-energy image. The recombined image is an adjunct to the low-energy image rather than a replacement.

As with breast MRI, background parenchymal enhancement (BPE) also occurs with CEM and should be evaluated. Sogani et al. performed a retrospective study of 278 women (aged 25–76 years) comparing BPE on CEM with that on breast magnetic resonance imaging (MRI) [9]. Three readers independently scored BPE as minimal, mild, moderate, or marked on CEM and MRI in the same patients. Most women had minimal or mild BPE on both CEM (68–76%) and breast MRI (69–76%), and there was good agreement between CEM and MRI. Both modalities showed a significant association between BPE and menopausal status, prior breast radiation therapy, hormonal treatment, and breast density.

Although no studies to date have studied the effect of BPE on CEM accuracy, one might consider that for elective CEM exams, i.e., screening, similar guidelines should be applied as breast MRI to reduce the presence of BPE [10]. For breast MRI, the exam is ideally performed in the first phase of the menstrual cycle (i.e., days 3–14), with day 1 being the first day of menstruation [11]. Institutes that adhere to these guidelines for MRI would probably apply the same for CEM. However, evidence of improved breast MRI with these guidelines are conflicting. As DeMartini et al. showed, although increased BPE in breast MRI is associated with a younger patient age and a higher abnormal interpretation rate, it was not related to significant differences in positive biopsy rates, cancer yield, sensitivity, or specificity [12]. Hence, some institutes might prefer not to consider the menstrual cycle when planning elective (screening) CEM exams. In other CEM indications, the exam should be performed at the earliest opportunity. In these cases, rapid clarification through imaging is preferred over optimal BPE in CEM.

Finally, regarding the evaluation of BPE, the report of the recombined images should include a description of the BPE with special focus on the symmetry of BPE, as asymmetrical BPE could be caused by underlying invasive (lobular) breast cancer or ductal carcinoma in situ (without accompanying calcifications) (Fig. 4.7).

Any relevant enhancement on recombined images should be matched with findings on low-energy images. In some cases, no mammographic counterpart can be observed for areas of enhancement. Enhancement should be described as enhancement associated with an underlying mass or architectural distortion or as non-mass enhancement. In contrast to breast MRI, the term “focus” may not be applicable to CEM as enhancing lesions observed in two views should be called a mass, even if they are very small. For non-mass enhancement, similar terminology as breast MRI

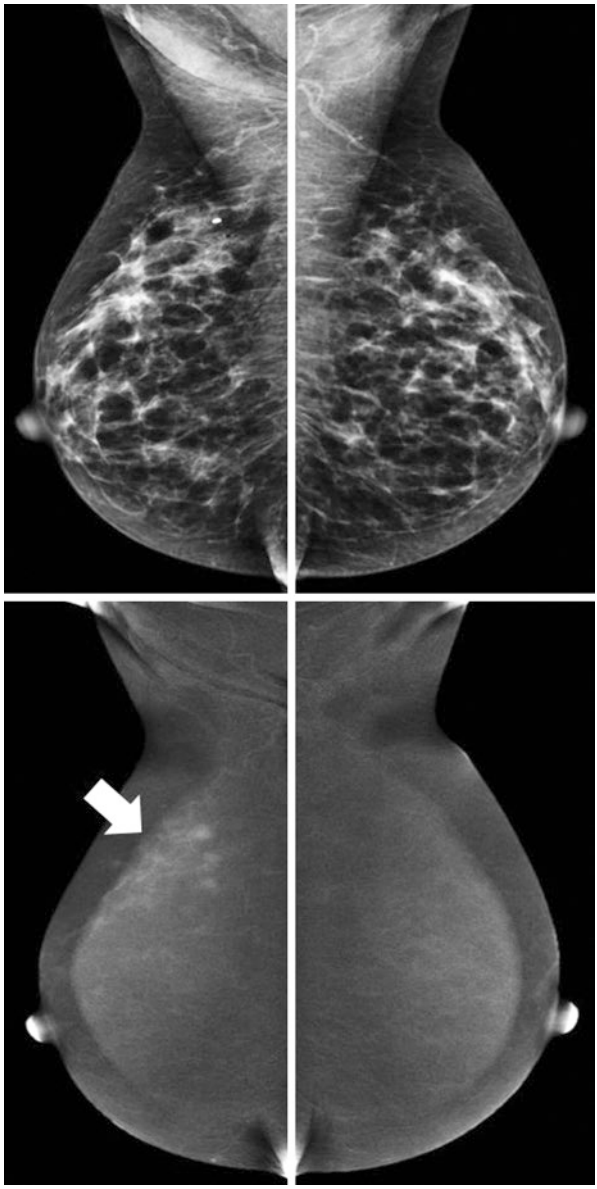

Fig. 4.7 Asymmetric enhancement might be the only sign of underlying breast cancer. In this case, asymmetrical non-mass enhancement in a segmental orientation was observed. Final diagnosis was a 6 mm invasive breast cancer with extensive ductal carcinoma in situ up to 60 mm

can be used to describe the orientation of the enhancement [7]. Non-mass enhancement can thus be focal, linear, segmental, regional, multiple regions, or diffuse.

Enhancement should also be assessed qualitatively, but there is not yet a single accepted classification for this purpose. Some institutes prefer a "yes/no" classification. Others prefer a more detailed classification and use "no/mild/moderate/marked." However, progress is being made to quantitatively assess CEM enhancement. Hwang et al. used a tool filled with fluid chambers on a known contrast agent

concentration [13]. Based on the linear relationship between contrast-to-noise levels measured and iodine concentrations, iodine overlay maps could be generated for the recombined images. In a single clinical case of a multifocal breast cancer, they calculated the enhancement of CEM (expressed as iodine mass thickness (IMT) in mg l/cm^2) for three different foci: 2.8, 1.5, and 1.3 mg l/cm^2. Parallel to this study, Lobbes et al. used a similar approach and calculated a mean IMT of 2.1 mg l/cm^2 (range 1.3–3.4 mg l/cm^2) for breast cancers [14]. In addition, they showed that malignant lesions enhanced more intensely than benign lesions. Therefore, it is expected that the rate of enhancement of lesions, when it can be accurately assessed, can be used to further improve the diagnostic accuracy of CEM, potentially even discriminating between breast cancer subtypes as Van Nijnatten et al. has shown that invasive lobular carcinomas more often show very weak enhancement [15]. Artificial intelligence and computer-aided decision systems could boost the accuracy of CEM potentially even more (see also Sect. 4.4).

When there is a significant discrepancy regarding the maximum diameter of the lesion between the low-energy and recombined images, this discrepancy should also be reported.

4.3.3 False-Negative Findings in CEM

Since the introduction of CEM in 2011, many studies have shown that the diagnostic accuracy of CEM is consistently superior to that of FFDM. These findings were summarized in a systematic review by Tagliafico et al., showing that the estimated sensitivity of CEM was 98%, with only a moderate specificity of 58% [16]. The latter could be explained by the overrepresentation of papers of a single study group within this review. Jochelson and Lobbes recalculated the results of this review and observed a specificity of 78% [17]. In an updated review, Zhu et al. reported a pooled sensitivity and specificity of 89% and 84%, respectively [18].

Prior studies have reported on "missed cancer diagnosis" when using CEM. Thibault et al. reported six missed cancers in their population of 54 patients, which were mostly invasive lobular cancers or cancer located outside of the mammographic field of view (caused by suboptimal patient positioning) [19]. Fallenberg et al. reported one cancer missed by all three readers (in a study population of 118 women) [1]. Lalji et al. reported ten missed cancers (overlooked by more than one reader in a study of ten readers in total) [20]. The main causes for the missed diagnosis were weak enhancement and location outside of the mammographic field of view.

4.3.4 CEM in the Evaluation of Suspicious Breast Calcifications

The diagnostic accuracy of CEM with respect to pathological calcifications was studied by Cheung et al. who reported a sensitivity and specificity of 89% and 87%, respectively [21]. These findings are like the findings by Houben et al. Of note,

Houben et al. found that the diagnostic accuracy of the complete CEM exam did not differ significantly from that of only low-energy images [22]. The sensitivity and specificity using only low-energy images were 91% and 39%, respectively. For the complete CEM exam, the sensitivity was 94%, while the specificity was 37%. In addition, Houben et al. evaluated the impact of using CEM to evaluate breast calcifications on surgical decision-making; they observed no relevant differences between low-energy images and a complete CEM exam. Hence, the added value of CEM for the evaluation of suspicious calcifications is limited and can only be used for upgrading lesions: when calcifications show enhancement, the likelihood of an underlying cancer increases, but biopsy of suspicious calcifications should be performed regardless of the lack of enhancement, just as with breast MRI.

4.3.5 Contamination Artifacts

Contamination artifacts mimicking suspicious breast calcifications have been reported by Gluskin et al. [23]. Contrast can be transported on the hands of the technologist, especially if gloves are not worn or if the line is not properly connected. Although the low-energy image does not demonstrate the presence of iodine within the breast, contamination of the skin with contrast might mimic calcifications due to the higher concentration of contrast agent, producing a greater attenuation of photons relative to the intravenous contrast distributed throughout the breast. The artifact can be recognized by viewing the recombined image in overlay of the low-energy image. Due to the subtraction algorithm used for the recombined images, "true" calcifications will appear black on recombined images. In case of contrast splatter, the "calcifications" will remain white on the recombined images (Fig. 4.8). This latter observation should trigger the radiologist to consider contrast contamination. Other warning signs are as follows: (1) the findings are observed in only one view or the mirror image of findings seen in another view or breast; (2) the abnormality does not persist on high-quality magnification views; and (3) the findings do not persist on repeat CEM studies [23]. Contrast contamination can be easily managed by cleansing, but technologists should be aware that contamination could occur on either the breast or the detector. Also, the risk of encountering this artifact is reduced by wearing gloves during patient handling, handwashing, and/or having contrast administration and mammographic positioning done by two different technologists.

4.4 Outlook and Future Perspectives

Reading CEM images does not require an extended training. When the radiologist viewing CEM exams is also experienced with reading both FFDM and breast MRI, there is no difference between the performance of expert CEM readers or experienced breast radiologists. This was demonstrated by a study by Lalji et al., who showed that the diagnostic accuracy among four experienced CEM readers was comparable to that of experienced breast radiologists [20]. Nevertheless, a

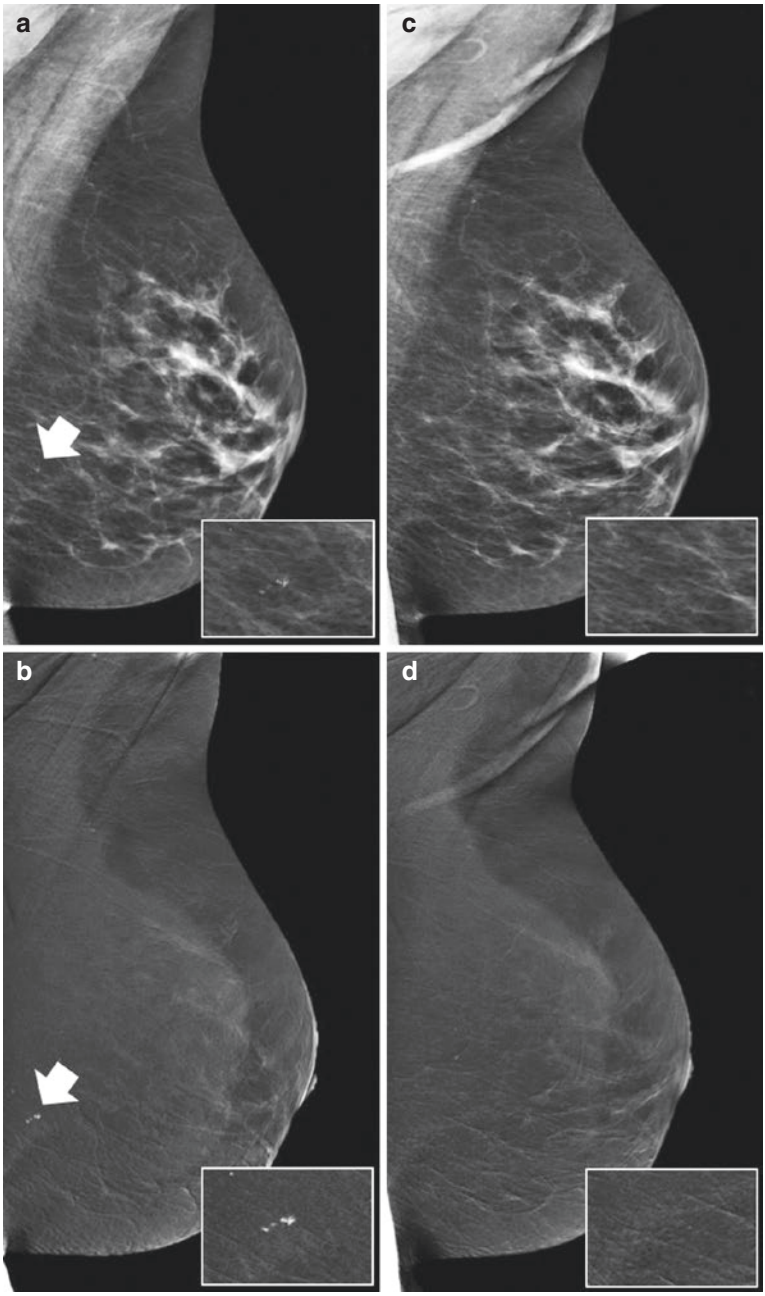

Fig. 4.8 Example of iodine contamination artifact. During this CESM exam, an area suspicious for pathologic micro calcifications was observed on the low-energy images of the left breast (**a**, white arrow). However, this area was high in opacity on the recombined images (**b**), not compatible with micro calcifications (which are black in the recombined images), but suggestive of iodine contamination on the detector. Next, the detector was cleaned and the exam repeated (**c**, **d**), confirming that this abnormality was indeed caused by iodine contamination during the exam

consistency in terminology is required. Although many descriptors of conventional mammography and breast MRI can be applied to CEM exams, there are some phenomena that are exclusive to CEM. Efforts should be made on introducing consistency in terminology.

We are only touching the surface of CEM applications, as it provides a window of opportunity for advanced imaging analyses (e.g., using computer-aided diagnosis (CAD), radiomic feature analysis, and artificial intelligence). For example, Patel et al. were the first to study the application of CAD-CEM on 50 breast lesions [24]. Their algorithm could correctly identify 45 out of these 50 lesions (accuracy 90%), while the radiologists in this study achieved an accuracy of 78% and 86%, respectively. Preliminary data from our own institute applying deep learning algorithms and radiomics to CEM showed promising results. In 112 patients, the deep learning algorithm achieved an AUC of 0.67 (95% confidence interval (CI) 0.51–0.82), with radiomic feature analysis achieving an AUC of 0.90 (95% CI 0.84–0.96) (Van Wijk, unpublished data). These examples show that the superior diagnostic accuracy of CEM over FFDM can be further enhanced when using advanced computer programs. This is a very exciting field of research which can only make the promising technique of CEM even more robust.

References

1. Fallenberg EM, Dromain C, Diekmann F, et al. Contrast-enhanced spectral mammography: does mammography provide additional clinical benefits or can some radiation exposure be avoided? Breast Cancer Res Treat. 2014;146:371–81.
2. Francescone MA, Jochelson MS, Dershaw DD, et al. Low energy mammogram obtained in contrast-enhanced digital mammography (CEDM) is comparable to routine full-field digital mammography (FFDM). Eur J Radiol. 2014;83:1350–5.
3. Lalji UC, Jeukens CR, Houben I, et al. Evaluation of low-energy contrast-enhanced spectral mammography images by comparing them to full-field digital mammography using EUREF image quality criteria. Eur Radiol. 2015;25:2813–20.
4. European Reference Organisation for Quality Assured Breast Screening and Diagnostic Services. EUREF European guidelines. 4th ed; 2013. http://www.euref.org/european-guidelines
5. Yagil Y, Shalmon A, Rundstein A, et al. Challenges in contrast-enhanced spectral mammography interpretation: artefacts lexicon. Clin Radiol. 2016;71:450–7.
6. Jeukens CR, Lalji UC, Meijer E, et al. Radiation exposure of contrast-enhanced spectral mammography compared with full-field digital mammography. Investig Radiol. 2014;49:659–65.
7. D'Orsi CJ, et al. ACR BI-RADS Atlas, breast imaging reporting and data system. Reston, VA: American College of Radiology; 2013.
8. Lobbes MB, Cleutjens JP, Lima Passos V, et al. Density is in the eye of the beholder: visual versus semi-automated assessment of breast density on standard mammograms. Insights Imaging. 2012;3:91–9.
9. Sogani J, Morris EA, Kaplan JB, et al. Comparison of background parenchymal enhancement at contrast-enhanced spectral mammography and breast MR imaging. Radiology. 2017;282:63–73.
10. Mann RM, Kuhl CK, Kinkel K, Boetes C. Breast MRI: guidelines from the European Society of Breast Imaging. Eur Radiol. 2008;18:1307–18.
11. Delille JP, Slanetz PJ, Yeh ED, et al. Physiologic changes in breast magnetic resonance imaging during the menstrual cycle: perfusion imaging, signal enhancement, and influence of the T1 relaxation time of breast tissue. Breast J. 2005;4:236–41.

12. DeMartini WB, Liu F, Peacock S, et al. Background parenchymal enhancement on breast MRI: impact on diagnostic performance. AJR Am J Roentgenol. 2012;198:W373–80.
13. Hwang YS, Cheung YC, Lin YY, Hsu HL, Tsai HY. Susceptibility of iodine concentration map of dual-energy contrast-enhanced digital mammography for quantitative and tumor enhancement assessment. Acta Radiol. 2018;59:893–901.
14. Lobbes MBI, Mulder H, Rousch M, et al. Quantification of enhancement in contrast-enhanced spectral mammography using a custom-made quantifier tool (I-STRIP): a proof-of-concept study. Eur J Radiol. 2018;106:114–21.
15. Van Nijnatten TJA, Jochelson MS, Pinker K, et al. Differences in degree of lesion enhancement on contrast-enhanced mammography between invasive lobular and ductal carcinoma. BMJ Open. 2019; Under review.
16. Tagliafico AS, Bignotti B, Rossi F, et al. Diagnostic performance of contrast-enhanced spectral mammography: systematic review and meta-analysis. Breast. 2016;28:13–9.
17. Jochelson M, Lobbes MBI, Bernard-Davila B. Reply to Tagliafico AS, Bignotti B, Rossi F, et al. Breast. 2017;32:267.
18. Zhu X, Huang JM, Zhang K, et al. Diagnostic value of contrast-enhanced spectral mammography for screening breast cancer: systematic review and meta-analysis. Clin Breast Cancer. 2018;18(5):e985–95.
19. Thibault F, Balleyguier C, Tardivon A, Dromain C. Contrast enhanced spectral mammography: better than MRI? Eur J Radiol. 2013;81(Suppl 1):S162–4.
20. Lalji UC, Houben IPL, Prevos R, et al. Contrast-enhanced spectral mammography in recalls from the Dutch breast cancer screening program: validation of results in a large multireader, multicase study. Eur Radiol. 2016;12:4371–9.
21. Cheung YC, Juan YH, Lin YC, et al. Dual-energy contrast-enhanced spectral mammography: enhancement analysis on BI-RADS 4 non-mass microcalcifications in screened women. PLoS One. 2016;11:e0162740.
22. Houben IPL, Vanwetswinkel S, Kalia V, et al. Contrast-enhanced spectral mammography in the evaluation of breast suspicious calcifications:diagnostic accuracy and impact on surgical management. Acta Radiologica. 2019; Jan 24, Epub ahead of print.
23. Gluskin J, Click M, Fleischman R, et al. Contamination artifact that mimics in-situ carcinoma on contrast-enhanced digital mammography. Eur J Radiol. 2017;95:147–54.
24. Patel BK, Ranjbar S, Wu T, et al. Computer-aided diagnosis of contrast-enhanced spectral mammography: a feasibility study. Eur J Radiol. 2018;98:207–13.